HYBRIDIZATION-CONTROLLED CHARGE TRANSFER AND INDUCED MAGNETISM AT CORRELATED OXIDE INTERFACES - SUPPORTING INFORMATION

A. Background correction

To correct for the La-peak we used a reference sample of GTO grown on LAO and capped by 7 unit cells LAO film on top of GTO. The conductivities of the samples are different and can lead to different absorption intensities due to charging effects in the samples. This can indeed induce very important issues such as strong discrepancies in the L_2/L_3 intensities ratio depending on the flux. However, in this case charging effects appear negligible and the difference between LNO/GTO and LAO/GTO conductivities is minimal. We then apply a constant factor to the LAO/GTO absorption spectrum (shown in black) to scale that of the LNO/GTO (shown in red). The subtraction of the two signals gives the corrected spectrum presented in blue, which does not show a strong contribution of the La-peak. Note that in case of charging effect due to the incident beam and to the poor conductivity, the spectral shape may be changed but this is clearly not the case in our analysis where the two signals scale almost perfectly.

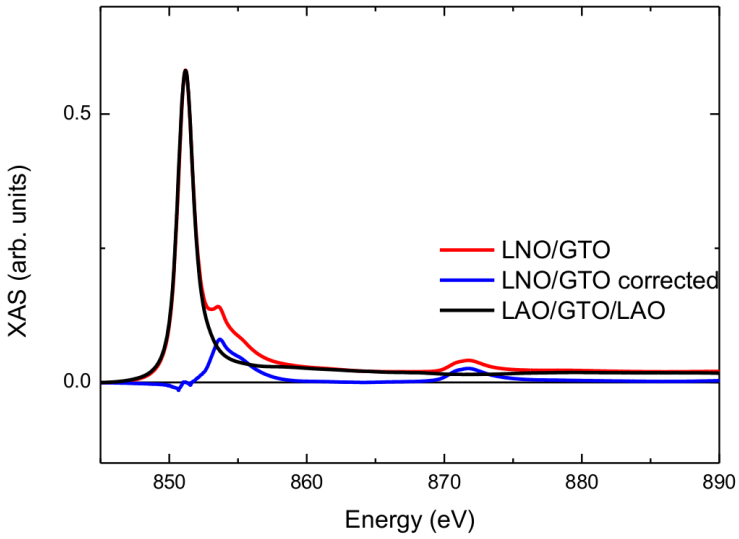

Figure SI 1. Correction of the Ni L-edge data from the La-M peak.

B. HXPS analysis

To know precisely at which position the HXPS analysis was performed, we performed simulation of the photon field distribution in the sample depending on the incident beam angle. The distribution is presented in Fig SI 2

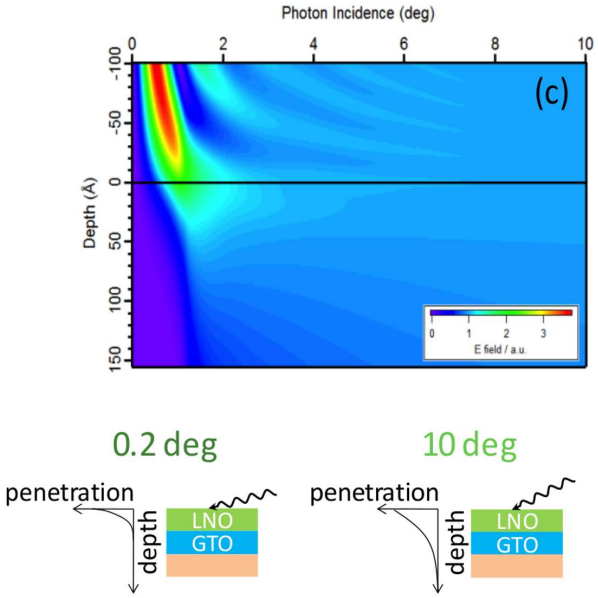

Figure SI 2. Photon field distribution in the sample as a function of the incident beam angle.

In addition, the analysis of the Ti HXPS thickness analysis requires more details. Both spectra (cyan and dark blue) shown in Fig. 2d suggest Ti $2p_{3/2}$ core-level is made of at least two components separated by 1.1 eV, with the component at low binding energy being enhanced at 0.2 deg. This separation is much smaller than that expected between pure Ti^{4+} and Ti^{3+} peaks (typically >2 eV) (see Refs. SI 1 and 2). In addition, there are differences in the absolute binding energy values: in the references mentioned above, the Ti^{4+} peak occurs at 459.5 eV and that of Ti^{3+} at 457.5 eV. In our case, the high binding energy peak occurs at about 458.2 eV and the low binding energy peak at about 457.1 eV. This suggests that the Ti valence is mostly 3+, and that an additional mechanism causes the spectra to show different components. We argue that the increase of the signal at low binding energies at 0.2 deg (the configuration which is most sensitive to the interface region) reflects the presence of a built-in electric field shifting the core levels of interfacial Ti ions to higher energies (i.e. to lower binding energies) near the interface.

C. Valence Band HXPS in nickelates

Fig SI 3.a shows valence band HXPS of a single films of $LaNiO_3$ in surface and bulk detection modes. The bulk signal is very typical of valence band photoemission of this material (Refs. SI 3 and 4) and the peaks corresponding to t_{2g} and e_g states are easily recognizable. At the surface, the intensity of those two peaks is reduced, which possibly reflects some reduced metallicity. This is better visualized in Fig SI 3.c that plots the difference between bulk and surface signals.

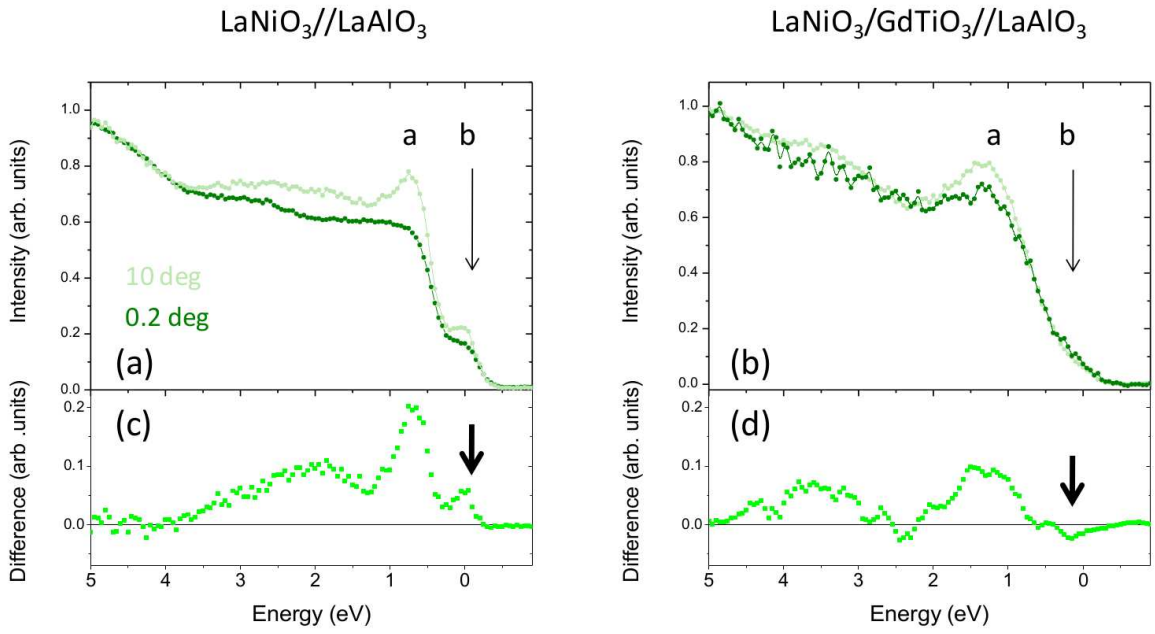

Figure SI 3. Valence Band Hard X-ray Spectroscopy in nickelate thin film and bilayerLNO/GTO.

Fig SI 3.b shows similar data for the LNO/GTO bilayer. Compared to data from Fig SI 3.a, the t_{2g} peak appears broader and the e_g is much less intense. Such a progressive weakening of the quasiparticle peak and the depletion of spectral weight at the Fermi level has been observed for LNO in the 3 to 6 unit-cell thickness range (close to the thickness of our LNO films, 7 unit-cells). The t_{2g} is further weakened at the surface mode compared to the bulk (as in the LNO single film), but what is remarkable is that the e_g peak is now weaker in bulk that in surface (this is clearly visible from the difference plotted in Figure 3.d, that is negative at the e_g peak). This suggests a transfer of spectral weight to lower energies consistent with an increase in the number of electrons, in other words a reduction of the Ni valence from 3+ to 2+. Because here HAXPS is more sensitive to the interface GTO in bulk mode than in surface mode, this suggests a change of the Ni valence

towards 2+ near the interface.

D. First-principles study of oxide interfaces

Technical details

In order to simulate bilayers, we used a $(GdTiO_3)_n/(RNiO_3)_n$ superlattices (n equals 1 to 7) assuming a growth along the [001] *Pbnm* direction for both subsystems as pictured in Fig SI 4. This superlattice approach allows us to avoid surface effects, and therefore to use dipole and quadrupole corrections in our simulations. During the geometry optimization, atomic positions and lattice parameters were relaxed, except the $\vec{a}$ and $\vec{b}$ lattice vectors fixed to the imposed parameters by the $LaAlO_3$ substrate. The oxygen cage rotations were imposed to a $a^-a^-c^+$ pattern as defined in Glazer's notation (Ref. SI 5. This additional constraint allows us to reduce as much as possible the computational cost of the simulations.

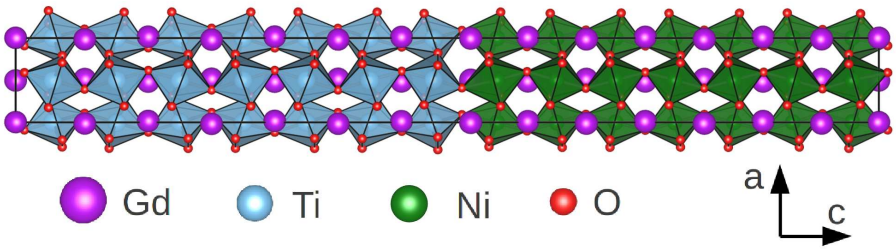

Figure SI 4. $(GdTiO_3)_n/(GdNiO_3)_n$ superlattice (n=7) used during the calculations. The growth direction is assumed to be along the [001] *Pbnm* direction for both subsystem.

As addressed by Picket *et al* (Ref. SI 6), and discussed in Refs. SI 7 and 8 for instance, the charge degree of freedom is ill-defined in DFT calculations as there is not an unique method to separate charge between species. For instance, our calculations on bulk nickelate ($P2_1/n$ symmetry), in line with previous study (Ref. SI 8), reveal no charge ordering between the two distinct nickel sites, even though experiments show a charge ordered state. However, the magnetic moment between the two nickel sites in our calculations exhibits a "spin charge ordering", reflecting the actual charge ordering degree of freedom appearing in nickelates. The magnetic moment quantity is indeed a localized quantity and is therefore well defined and reliable for spin polarized systems (Ref. SI 6). Hence, we rely on this quantity to access the number of electrons transferred across the interface between titanates and nickelates, and also for the covalence analysis in nickelates. In order to

include strain effects, the reference magnetic moments were set to both $GdTiO_3$ and $GdNiO_3$ grown on a $LaAlO_3$ substrate.

Covalence of bulk nickelates

We performed full geometry relaxations of bulk nickelates in order to access covalence effect in their ground state. In the case of $GdNiO_3$, we identify a S-type antiferromagnetic ground state with two distinct magnetic moments: one Ni site holds a magnetic moment of 1.237 μ_B per Ni while the second site exhibits a zero magnetic moment, in line with previous DFT+U studies (Refs. SI 8 and 9), as well as a hybrid functional study (Ref. SI 10). Fig SI 5 (left panel) displays the density of states of $GdNiO_3$ ground state projected on two distinct Ni sites (total d-orbitals contribution) and on a bridging O atom (total p-orbitals contribution) in a NiO_2 plane. We observe a strong hybridization between the Ni d-orbitals and O p-orbitals, revealing the highly covalent character of nickelates. We also a observe two peaks below the Fermi level (between -0.5 eV and 0 eV),

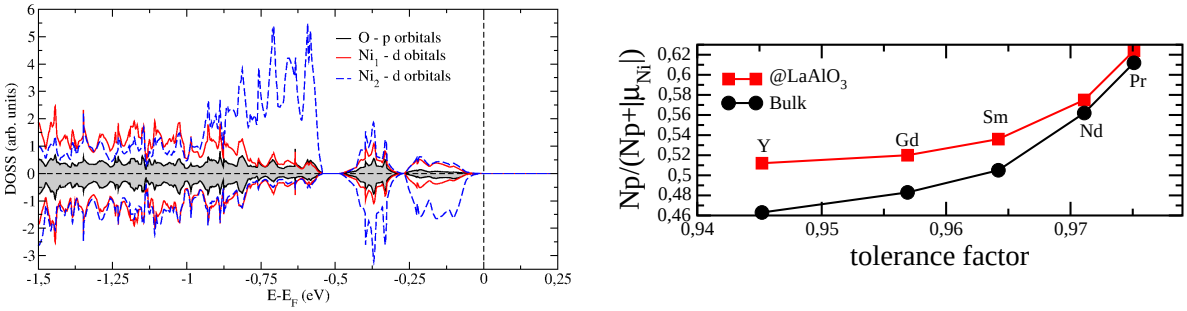

Figure SI 5. Left panel: Projected density of states of $GdNiO_3$ on the total d-orbitals of the two distinct Ni sites (dashed blue and solid red curves) and on the total p-orbitals of one bridging O in the NiO_2 plane (solid black and grey filled curves); right panel: Covalence extracted from our first principles calculations on several bulk nickelates (black filled circles) and when grown on a $LaAlO_3$ substrate (red filled squares).

well separated from deeper levels. We tried to extract the covalence by evaluating how much the resulting magnetic moment of Ni sites from these two peaks spreads on oxygen contributions (Ref. SI 13). In other words, our extracted covalence is defined as

$$\text{covalence} \propto \frac{\text{N-p electrons}}{\text{N-p electrons} + |\mu_{Ni}|} \tag{1}$$

We performed this analysis for various bulk nickelates, and also for strained nickelates when grown on a $LaAlO_3$ substrate in order to access the strain effect (see Fig. SI 5 right panel). The trend of the covalence with respect of tolerance factor is non linear. For small tolerance factor, it slightly

increases (Y and Gd) and then strongly increases for large tolerance factor (Sm, Nd and Pr). It would probably reach its maximum for $LaNiO_3$ if such an analysis could be performed for this latter compound. When grown on a $LaAlO_3$ substrate, the trend of the covalence as a function of the tolerance factor is rather similar to the bulk behaviour, even if is slightly increased for the smallest tolerance factor (Y, Gd and Sm). In conclusion, even grown on a $LaAlO_3$ substrate, the trend of covalence with respect to the rare-earth is not strongly affected, and the trend of the experimentally observed charge transfer for various rare-earth in $(GdTiO_3)_7/(RNiO_3)_7$ bilayers couldn't be ascribed to strain effect.

Charge Transfer at oxide interfaces: insights from DFT calculations

We performed geometry relaxations on a set of $(GdTiO_3)_n/(GdNiO_3)_n$ superlattices ($n \leq 7$) in order to get insights on the charge transfer across the interface between the titanate and the nickelate. This system constitutes an ideal one as the environment between Ti and Ni atoms is similar and no built-in polarization altering the charge transfer exists. All lattice distortions were allowed during the relaxation, including the breathing of the oxygen cage linked to the charge disproportionation in nickelates. Firstly, the charge transfer is mainly localized at the interface in the $GdTiO_3$ subsystem while it spreads on 3 unit cells in $GdNiO_3$, eventually with a strong contribution coming from the interfacial plane. We measure a charge transfer of around 0.85 electron across the interface. At the interface, the resulting magnetic moment of the Ti cation is around 0.12 μ_B, going towards a Ti^{4+} state. Beyond the interface, all Ti cations recover their bulk magnetic moment (0.93 μ_B) indicating that they are in a Ti^{3+} configuration. Regarding the nickelates, the average magnetic moment per Ni in the interfacial layer is around 1.47 μ_B. This value is very close to the value we compute in Li_2NiO_2 (1.58 μ_B) using similar U parameters, in which all Ni are in a 2+ oxidation state. This indicates a dominant Ni^{2+} character at the interfacial layer. The Ni in the next two layers develop a slightly larger magnetic moment (0.94 μ_B per Ni) than the bulk (0.86 μ_B per Ni). At the fourth layer, the bulk behaviour is recovered. In summary, our DFT calculations predict a large charge transfer, mainly at the interface, with a local change on Ti and Ni towards Ti^{4+} and Ni^{2+} respectively. We emphasize that the charge ordering develops in the nickelate after the interfacial layer, if the system is large enough (n>5). Finally, it is worth noting that removing the breathing of the oxygen cage does not alter the charge transfer (the amount of transferred electrons is identical).

Factors affecting the amount of charge transferred

We tried to extract from our calculations the factors affecting the amount of charge transferred across the interface. Since the charge transfer is mainly located at the interface, we performed this study only on a $(GdTiO_3)_1/(GdNiO_3)_1$ system for computational cost. We again chose the same R cation in both subsystem in order to avoid polar structures, and also this system should develop large lattice distortions due to a relatively small tolerance factor. Lattice distortions were extracted using Amplimodes from the Bilbao Crystallographic server (Refs. SI 11 and 12). The ground state of this (1/1) superlattice exhibits three main distortions: two antiferrodistortive (AFD) motions ($a^-a^-c^0$ and $a^0a^0c^+$ oxygen cage rotations) and one anti-polar X_5^- motion whose atomic displacement is in the (xy)-plane. We then condensed individually the different distortions in an ideal cube on cube $P4/mmm$ structure and we extracted the variation of the magnetic moment in both subsystems (see Fig SI 6 left panel). As discussed in the technical part, this variation is homogeneous to a variation of electron transferred between the titanate and the nickelate. We

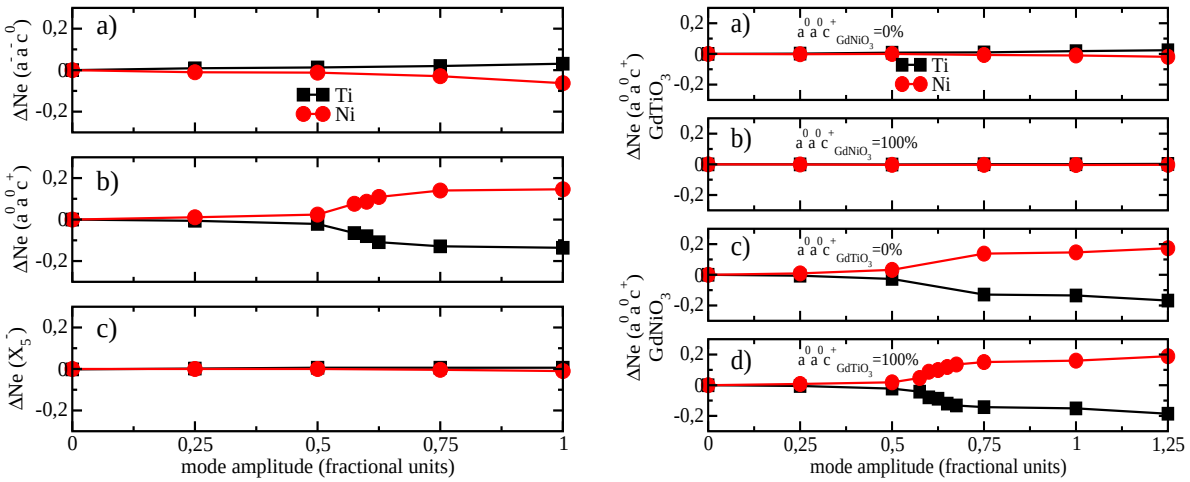

Figure SI 6. Left panel: Influence of the three main distortions appearing in a $(GdTiO_3)_1/(GdNiO_3)_1$ superlattice on the amount of charge transferred between the titanate and the nickelate: the $^-a^-c^0$ AFD motion (top panel), the $a^0a^0c^+$ AFD motion (middle panel) and the anti-polar X_5^- motion (bottom panel); right panel: Influence of the $a^0a^0c^+$ rotation in $GdTiO_3$ or $GdNiO_3$ by imposing 0% (a/c) or 100% (b/d) of this distortion in the nickelate or titanate respectively.

identify that the anti-polar X_5^- and especially the $a^-a^-c^0$ AFD motions have nearly no effect on the charge transfer across the interface, whatever their magnitude are in the structure. Eventually, tuning the $a^0a^0c^+$ AFD motion may tune in consequence the number of electron transferred between the two subsystems. This may be achieved by changing the rare-earth involved in the system, hence

changing the covalent character of the nickelate.

We then checked the independent role of the $a^0a^0c^+$ oxygen cage rotations in both subsystems by fixing this latter in one subsystem and freezing-in some amplitude in the other subsystem (see Fig SI 6 right panel). The oxygen rotation cage in the titanate has clearly no impact on the amount of charge transferred, whatever the magnitude of the AFD motion is in the nickelate. The trend is totally different for the nickelate $a^0a^0c^+$ rotation. Indeed, as the magnitude of this rotation increases, the amount of electron transferred increases, whatever the magnitude of the rotation is in the titanate. This results totally demonstrates that tuning the sole rotation in the nickelates, by R-cation substitutions, may alter the charge transfer, independently of the rotation in the titanates. Since the $a^0a^0c^+$ AFD motion might tune the covalence of the nickelate (as the tolerance factor increases, the $a^0a^0c^+$ may decrease), this observation totally supports the covalence-controlled charge transfer observed in the main manuscript, both from experiments and calculations.

Termination effect

Finally, we considered the effect of the termination on the charge transfer. From a pure charge analysis, it may not play a major role in the covalence control of charge transfer. Indeed, whatever the termination is, the charge configuration is exactly the same and no polar interface exists: $(GdO)^+$-$(TiO_2)^-$-$(RO)^+$-$(NiO_2)^-$ or $(GdO)^+$-$(TiO_2)^-$-$(GdO)^+$-$(NiO_2)^-$-$(RO)^-$. However, we checked the two type of interfaces using our DFT calculations on a set of $(RTiO_3)_2/(RNiO_3)_2$ superlattices (R=Y, Gd, Sm, Nd), while taking care of not creating an artificial polarization through R-cation asymmetry. The system with n=2 constitutes the minimal size needed to simulate both interfaces. We also emphasize for the system with similar interface (*i.e* $(RO)^+$-$(TiO_2)^-$-$(RO)^+$-$(NiO_2)^-$, see Fig SI 7.a) that we intentionally restricted ourselves to one R cation in the whole system. This restriction is justified through our analysis demonstrating that only the $a^0a^0c^+$ rotation in the nickelate alter the charge transfer and it avoids any annihilation of nickelate's rotation magnitude from the titanate one (see Ref. SI 14). For the asymmetric interfaces (*i.e* $(GdO)^+$-$(TiO_2)^-$-$(RO)^+$-$(NiO_2)^-$, see Fig SI 7.b), the effect is sizeable as the rotation of the nickelate propagates in the titanate. Fig SI 7 evidenced that the termination has no impact on the trend of amount of charge transferred across the interface, despite it is slightly decreased in the case of

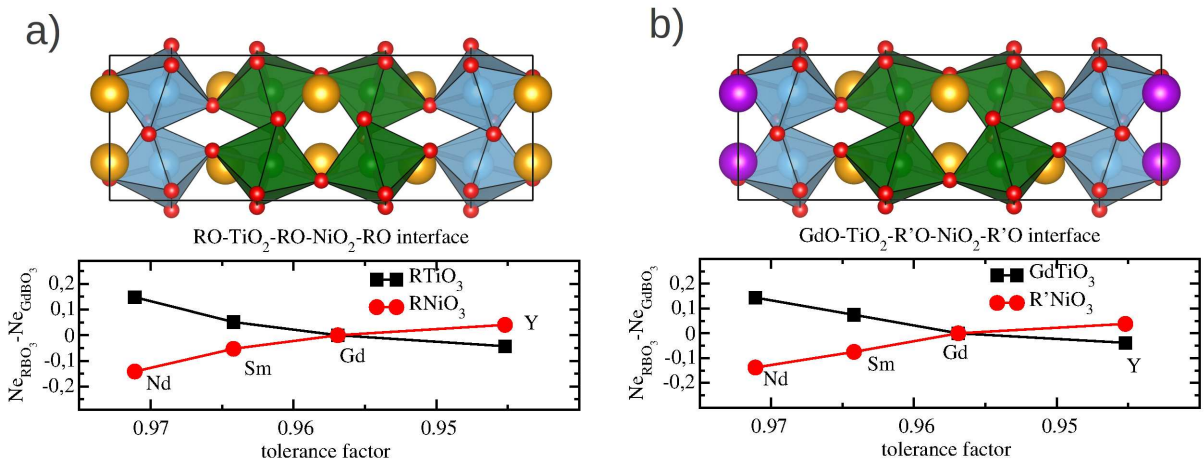

Figure SI 7. Termination effect on the charge transfer in the case of symmetric interfaces (a) or asymmetric interfaces (b).

asymmetric interfaces.

[1] M. Sing, G. Berner, K. Go, A. Müller, A. Ruff, A. Wetscherek, S. Thiel, J. Mannhart, S. A. Pauli, C. W. Schneider, P. R. Willmott, M. Gorgoi, F. Schäfers and R. Claessen, Phys. Rev. Lett. **102**, 176805 (2009).

[2] J. E. Rault, J. Dionot, C. Mathieu, V. Feyer, C. M. Schneider, G. Geneste and N. Barrett, Phys. Rev. Lett. **111**, 127602 (2013).

[3] E. Sakai, M. Tamamitsu, K. Yoshimatsu, S. Okamoto, K. Horiba, M. Oshima, and H. Kumigashira, Phys. Rev. B **87**, 075132 (2013).

[4] P. D. C. King, H. I. Wei, Y. F. Nie, M. Uchida, C. Adamo, S. Zhu, X. He, I. Boović, D. G. Schlom, and K. M. Shen, Nature Nano. **9**, 443 (2014).

[5] A. Glazer, Acta Cryst. B **28**, 3384 (1972).

[6] Y. Quan, V. Pardo, and W. E. Pickett, Phys. Rev. Lett. **109**, 216401 (2012).

[7] N. C. Bristowe, J. Varignon, D. Fontaine, E. Bousquet, and P. Ghosez, Nat. Commun. **6**, 6677 (2015).

[8] S. Prosandeev, L. Bellaiche and J. Íñiguez, Phys. rev. B **85**, 214431 (2012).

[9] H. Park, A. J. Millis and C. A. Marianetti, Phys. Rev. Lett. **109**, 156402 (2012).

[10] F. Y. Bruno, K. Z. Rushchanskii, S. Valencia, Y. Dumont, C. Carrétéro, E. Jacquet, R. Abrudan, S. Blügel, M. Leźaić, M. Bibes and A. Barthélémy, Phys. Rev. B **88**, 195108 (2013).

[11] D. Orobengoa, C. Capillas, M. I. Aroyo, and J. M. Perez- Mato, J. App. Cryst. **42**, 820 (2009)

[12] J. Perez-Mato, D. Orobengoa, and M. Aroyo, Acta Cryst. A **66**, 558 (2010).

[13] We used the magnetic moment of Ni to extract the covalence as the charge is ill-defined in DFT, especially in the case of covalent systems. For O atoms, as they are not spin polarized, we used the total amount of electrons.

[14] Indeed, in order to have symmetric interfaces preserving the $GdTiO_3$ subsystem, one needs three GdO layers against one RO layer. However, this forces the rotation in the nickelate to a similar magnitude as the one developed in the titanate. Therefore, no effects are observed despite changing the R cation.